



Article

<https://doi.org/10.1038/s44220-026-00585-w>

Polygenic score for C-reactive protein is linked to faster cortical thinning and psychopathology risk in adolescents

Received: 4 June 2025

Accepted: 7 January 2026

Published online: 16 February 2026

Haixia Zheng ^{1,2}, Jonathan Savitz ^{1,2}, Ebrahim Haroon³, Jonathan Ahern ^{4,5}, Robert J. Loughnan ^{4,6}, Firas Naber¹, Bohan Xu^{1,4}, Katherine L. Forthman ¹, Robin L. Aupperle^{1,2}, Leanne M. Williams ⁷, Martin P. Paulus ^{1,2}, Chun Chieh Fan ^{1,4,8} & Wesley K. Thompson^{1,4}

Check for updates

Adolescence is a sensitive period of brain development marked by rapid cortical thinning and increased risk for psychiatric disorders, yet the biological drivers of atypical trajectories remain unclear. Here, using longitudinal data from the Adolescent Brain Cognitive Development Study, we examined whether genetic predisposition to systemic inflammation, indexed by polygenic scores for C-reactive protein (PGS-CRP), influences brain development and psychopathology. Higher PGS-CRP was associated with accelerated cortical thinning, particularly in medial temporal and insular regions, and with increased externalizing symptoms. Early-life infections independently predicted greater depressive and externalizing symptoms but did not interact with genetic risk. Mediation analyses indicated that cortical thinning partially accounted for the association between PGS-CRP and externalizing psychopathology. Biological annotation further identified the regional similarity between cortical effects of PGS-CRP and several neurotransmitter systems. Together, these findings suggest that genetic susceptibility to inflammation may shape adolescent brain maturation and contribute to mental health vulnerability via neuroimmune pathways.

Adolescence is an important neurodevelopmental period during which rapid cortical structure change occurs^{1–3} and when many psychiatric disorders begin to emerge⁴, suggesting that deviation from typical neuroanatomical development may partially underpin worse mental health outcomes in this sensitive age range. Among magnetic resonance imaging (MRI)-derived brain structural measures, cortical thickness exhibits a well-characterized, monotonic reduction across adolescence^{1,2}, reflecting key neurodevelopmental processes such as

synaptic pruning, myelination, neurogenesis and synaptogenesis^{3,5–8}. By contrast, cortical surface area and gray-matter volume exhibit more dynamic and regionally variable trajectories, showing nonlinear patterns with periods of expansion, plateau or decline depending on age, sex and cortical region^{3,9,10}. Recent large-scale longitudinal imaging studies suggest that cortical thinning is the dominant and most developmentally sensitive MRI marker during adolescence^{3,9,10}. Aberrant patterns of cortical thickness change over time, especially accelerated

¹Laureate Institute for Brain Research, Tulsa, OK, USA. ²Oxley College of Health and Natural Sciences, The University of Tulsa, Tulsa, OK, USA. ³Department of Psychiatry and Behavioral Sciences, Emory University School of Medicine, Atlanta, GA, USA. ⁴Center for Population Neuroscience and Genetics, Tulsa, OK, USA. ⁵Department of Cognitive Science, University of California, San Diego, La Jolla, CA, USA. ⁶J. Craig Venter Institute, La Jolla, CA, USA. ⁷Psychiatry and Behavioral Sciences, Stanford University School of Medicine, Palo Alto, CA, USA. ⁸Department of Radiology, University of California School of Medicine, San Diego, CA, USA. e-mail: HZheng@laureateinstitute.org

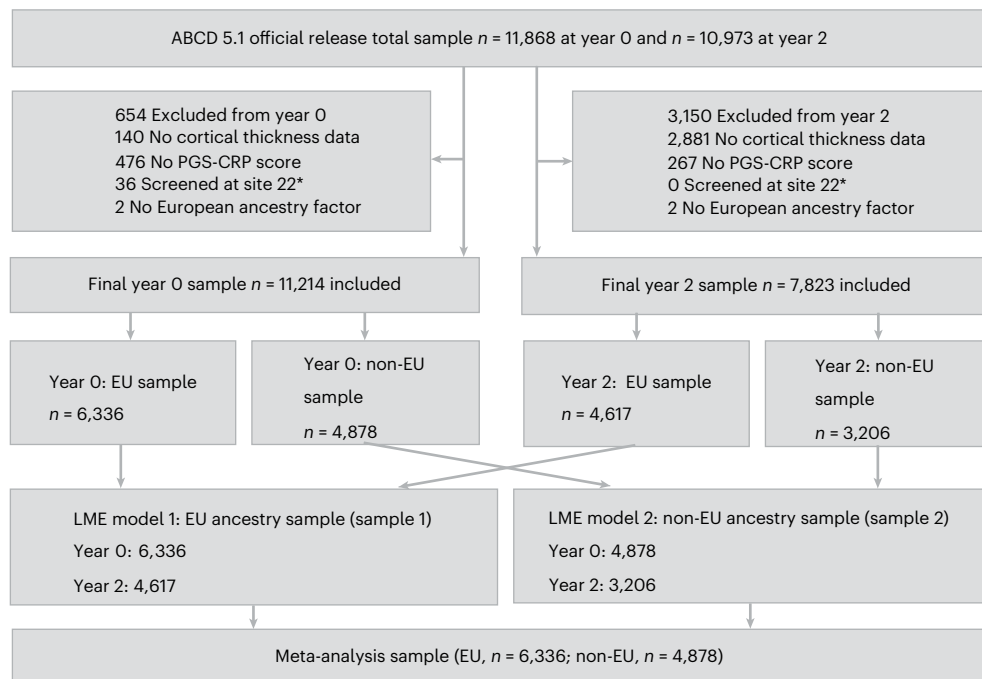


Fig. 1 | Participant flow and analytic sample derivation. Flowchart illustrating inclusion and exclusion of participants from the ABCD Study release 5.1 (total $n = 11,868$). Following quality control for cortical thickness and polygenic score (PGS-CRP) data, 6,336 European ancestry (EU) and 4,878 non-European ancestry

(non-EU) participants remained at year 0. At year 2, follow-up data were available for 4,617 EU and 3,206 non-EU participants. Ancestry groups were analyzed separately using LME models and combined via meta-analysis. *Site 22 was excluded because it withdrew from the ABCD Study.

thinning in frontal regions, are associated with worse cognitive and psychopathological outcomes in adolescents^{11–15}. However, the upstream biological factors that drive the deviation from typical cortical thinning process remain poorly understood. Identifying these factors and their interactions is critical for understanding the origins of mental health disorders that often arise during the sensitive developmental period of adolescence.

Emerging evidence suggests that immune signaling may play a key role in neurodevelopment. The neurodevelopmental processes underlying cortical thickness change (that is, synaptic pruning, myelination, neurogenesis and synaptogenesis^{3,5–8}) are highly susceptible to immune activation, which can result in lasting alterations in neural circuitry and brain function^{7,16,17}. At a cellular level, immune activation influences cortical development via glial cells, such as astrocytes and microglia. These glial cells not only support neuronal health but also actively participate in synaptic pruning and neural circuit formation^{18,19}. Inflammatory signals originating in the periphery can reach the brain via multiple pathways, including cytokine transport across the blood–brain barrier, vagal nerve signaling and monocyte trafficking²⁰, altering microglia activation²¹. These interactions also potentially disrupt neurotransmitter systems (for example, serotonin, dopamine and glutamate) and perturb neurocircuits involved in mood regulation²⁰. Indeed, neuroimaging studies have consistently shown that inflammation is associated with disrupted brain circuits integral to motivation, emotion regulation and cognitive processing²². Consistent with these mechanistic links, genetic and epigenetic studies have suggested that inflammation-related genetic profiles may influence risk for externalizing and internalizing psychopathology during childhood and adolescence by shaping neurocognitive development^{12,23,24}.

C-reactive protein (CRP), an acute-phase protein synthesized by the liver, is one of the most widely studied peripheral markers of systemic inflammation. CRP levels are a downstream acute-phase reactant that integrates multiple upstream cytokine pathways (for example, interleukin-6, interleukin-1 β and tumor necrosis factor)^{25–27} and exhibits strong correspondence between peripheral and central

concentrations ($r = 0.855$)²⁸, potentially explaining why peripheral CRP concentration has been associated with structural brain alterations^{29,30} and various psychiatric disorders, including major depressive disorder^{31,32}, bipolar disorder³³ and schizophrenia³⁴. While circulating CRP levels reflect active inflammation at a specific time point, they are also influenced by non-specific factors, such as socioeconomic disparities, age, body mass index, smoking and sleep disturbance, making direct comparisons of inflammation challenging³⁵. By contrast, the polygenic score for CRP (PGS-CRP)—a weighted sum based on an individual's genotype that quantifies genetic predisposition for elevated CRP levels—provides a static estimate capturing an individual's risk for inflammation. By capturing the heritable component of CRP levels, PGS-CRP (explaining approximately 16% of the variance in plasma CRP levels) is less confounded by short-term environmental or behavioral influences³⁶. Moreover, CRP is the only inflammatory biomarker with sufficiently powered genome-wide association data (>500,000 participants) to support reliable polygenic scoring, making it the most robust and generalizable genetic proxy for systemic inflammatory activity³⁶. Recent work shows that higher PGS-CRP is associated with greater negative affect and anxiety symptoms in adult population cohorts ($N = 55,098$), underscoring its relevance for mood disorder risk³⁷. Thus, PGS-CRP provides a powerful genetic instrument to investigate how inherited pro-inflammatory tendencies influence brain development and psychiatric vulnerability.

In parallel, early-life infection provides an environmental index of immune challenge that may amplify vulnerability to psychopathology. Large epidemiological studies have found that childhood infections are associated with elevated risk of mood and psychotic disorders in adolescence and adulthood, with hospital-treated infections linked to up to a 62% higher risk of mood disorders later in life^{38,39}. Importantly, the first year of life represents a critical window of neuroimmune development, when the immune system and brain undergo rapid co-maturation⁴⁰. During this period, systemic infection may disrupt neural cell genesis and microglial programming, producing long-term alterations in brain development⁴¹. Supporting this, longitudinal cohorts have reported

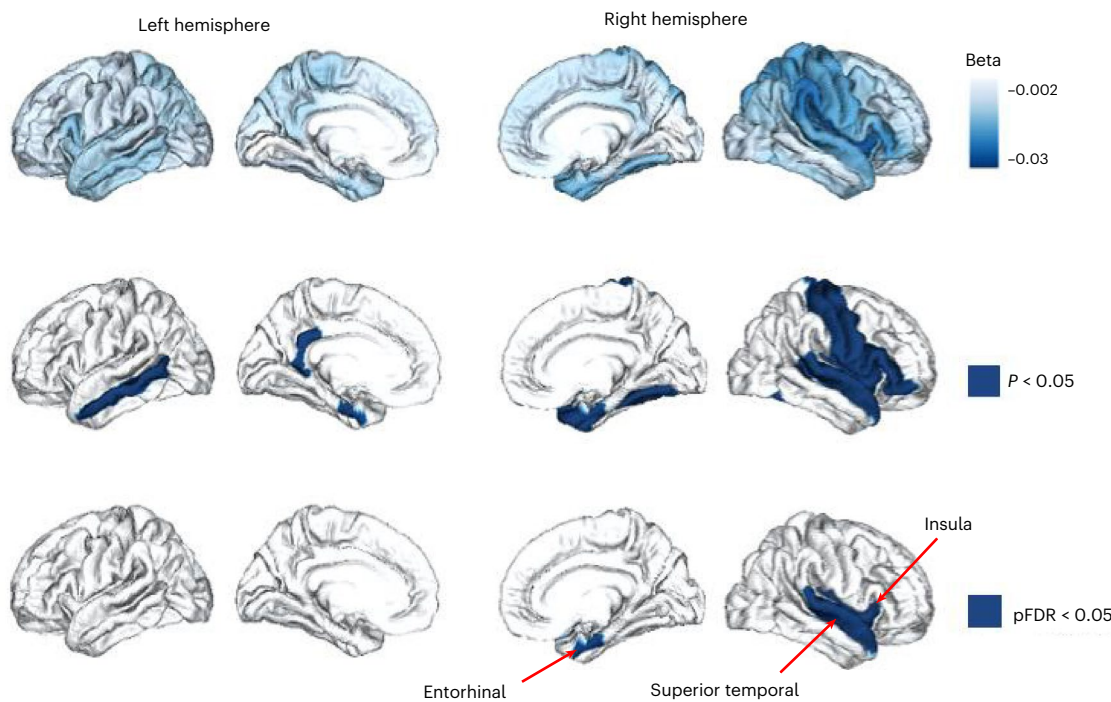


Fig. 2 | PGS-CRP is associated with variations in age-related cortical thinning during adolescence, with the strongest acceleration effect in the medial temporal lobe. This figure illustrates the interaction between PGS-CRP and age. The top row shows the standardized regression coefficients (β_3) for the interaction term (age \times PGS-CRP), with darker blue indicating stronger associations with accelerated cortical thinning. The middle row highlights regions where the interaction term was significant at meta-analysis $P < 0.05$,

and the bottom row identifies regions that survive FDR correction in the meta-analysis ($P_{\text{FDR}} < 0.05$). Statistical analysis used two-sided LME models with individual, family and site as random intercepts. Effects reflect standardized regression coefficients (β_3/β) from ancestry-stratified analyses, combined using inverse-weighted meta-analysis. Multiple comparisons across regions were controlled using Benjamini–Hochberg FDR. Exact P values and 95% confidence intervals are provided in Supplementary Table 1.

that infants exposed to antibiotic drugs in the first 2 years of life have been associated with greater risk for psychiatric diagnoses in later childhood⁴². For these reasons, our study focuses specifically on infection in the first year of life as an environmental predictor, complementing genetic liability for inflammation.

Taken together, both inherited and early environmental influences on inflammation may converge on neurodevelopmental pathways that confer risk for adolescent psychopathology. We therefore examine whether genetic liability to systemic inflammation (PGS-CRP) and early-life infection—individually and interactively—contribute to patterns of cortical thinning and emerging psychiatric symptoms in adolescence. We hypothesized that (1) greater genetic predisposition for elevated CRP levels is associated with an increased psychopathology risk and with altered patterns of cortical thinning, (2) genetic risk interacts with early-life infection to influence the psychopathology outcomes and cortical thinning process, and (3) neurobiological processes associated with cortical thinning partially mediate the relationship between genetic predisposition for high CRP levels and psychopathology. Finally, we explored whether the spatial pattern of cortical thinning overlaps with existing positron emission tomography (PET)-derived neurotransmitter receptor gradient maps, providing a biological annotation of the observed effects.

Results

Participants were stratified by imputed genetic ancestry into European and non-European samples to account for population stratification, and results were integrated using meta-analysis to enhance generalizability across diverse populations (Fig. 1). Statistical significance was determined using a false discovery rate (FDR) threshold of $P < 0.05$ based on meta-analysis results. See Methods for more details.

PGS-CRP effects on cortical thinning and psychopathology

The interaction term (β_3 ; see Methods ‘Statistical analyses’ for more details) allowed us to determine whether genetic predisposition for systemic inflammation, as captured by PGS-CRP, modifies age-related cortical thinning slopes. Meta-analytic findings across imputed ancestry groups revealed that higher PGS-CRP was significantly associated with steeper cortical thinning trajectories over 2 years across the brain cortex and particularly in medial temporal regions (Fig. 2). As shown in Fig. 2, three regions passed our statistical threshold (meta-analysis $P_{\text{FDR}} < 0.05$), including the right entorhinal cortex (PGS-CRP \times age interaction effect, $\beta_3 = -0.016$, $SE = 0.005$, $P_{\text{FDR}} < 0.05$), right insula cortex (PGS-CRP \times age interaction effect, $\beta_3 = -0.018$, $SE = 0.005$, $P_{\text{FDR}} < 0.05$) and right superior temporal gyrus (PGS-CRP \times age interaction effect, $\beta_3 = -0.013$, $SE = 0.004$, $P_{\text{FDR}} < 0.05$). These findings suggest that individuals in Adolescent Brain Cognitive Development (ABCD) with a higher genetic risk for systemic inflammation experience steeper cortical thinning trajectories in these regions over 2 years period. Regions that survived FDR correction are presented in Table 1, while the full set of results is available in Supplementary Table 1.

We observed a significant association between the PGS-CRP scores and externalizing psychopathology. Specifically, higher PGS-CRP scores were associated with greater externalizing symptoms at baseline, including behavioral problems such as aggression or rule-breaking (main effect of PGS-CRP on externalizing, $\beta_2 = 0.167$, $SE = 0.069$, $P_{\text{FDR}} = 0.048$). This suggests that genetic liability for systemic inflammation is associated with higher baseline levels of externalizing psychopathology, independent of age and early-life infection status. There were no significant main PGS-CRP effects on depression or internalizing psychopathology. The full set of results is available in Supplementary Table 2.

Table 1 | Brain regions with significant PGS-CRP by age interaction effects on cortical thinning

Regions	Data source ¹	β^2	SE ³	P	P_{FDR}
Right entorhinal cortex⁴	Meta analysis	-0.016	0.005	0.002	0.049
Right entorhinal cortex	EU sample	-0.019	0.007	0.008	0.493
Right entorhinal cortex	Non-EU sample	-0.014	0.008	0.098	0.308
Right insula cortex	Meta analysis	-0.018	0.005	0.001	0.049
Right insula cortex	EU sample	-0.016	0.007	0.028	0.493
Right insula cortex	Non-EU sample	-0.021	0.008	0.010	0.104
Right superior temporal gyrus	Meta analysis	-0.013	0.004	0.002	0.049
Right superior temporal gyrus	EU sample	-0.012	0.005	0.024	0.493
Right superior temporal gyrus	Non-EU sample	-0.015	0.007	0.026	0.139

¹Participants were stratified by genetic ancestry into two groups to address population stratification: individuals of European ancestry (EU sample) and non-European ancestry (non-EU sample). LME models were performed separately in each group, and a meta-analysis was conducted to integrate findings across both groups. Statistical significance was determined through meta-analysis, with a threshold of $P < 0.05$ after FDR correction. ² β , beta coefficient of PGS-CRP by age interaction effect on cortical thickness. ³SE, standard error. ⁴Bolded rows indicate statistically significant results ($P_{FDR} < 0.05$).

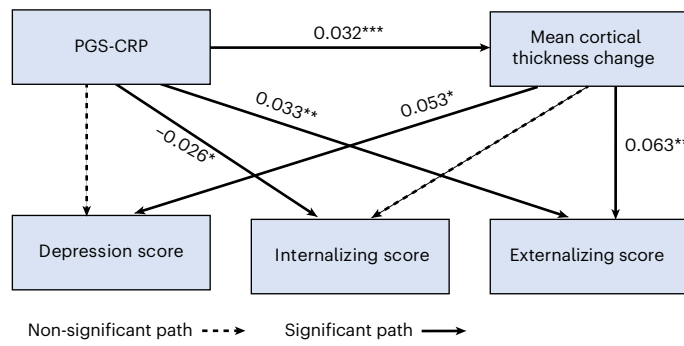
Early-life infection effects on cortical thinning and psychopathology

Meta-analysis showed no significant effects of early-life infection on cortical thickness at baseline (β_4), nor any interaction with age (β_5), PGS-CRP (β_6) or the 3-way interaction with age (β_7), indicating that early-life infection did not alter cortical thinning trajectories. By contrast, participants who had reported history of early-life infection exhibited significantly higher baseline depression scores (main effect of early-life infection, $\beta_4 = 0.511$, SE = 0.232, $P_{FDR} = 0.042$) and higher baseline externalizing psychopathology ($\beta_4 = 0.589$, SE = 0.232, $P_{FDR} = 0.034$). The association between early-life infection and internalizing psychopathology at baseline was not significant ($\beta_4 = 0.608$, SE = 0.363, $P_{FDR} = 0.094$). No interactions involving early-life infection (β_5 – β_7) were significant for any psychopathology outcomes. Detailed results are available in Supplementary Table 3.

Mediation pathways

The structural equation modeling was used to determine mediation pathways, and it demonstrated excellent fit: comparative fit index = 1.00, Tucker–Lewis index = 1.00 and standardized root mean square residual = 0.000, indicating no significant misfit. As shown in Fig. 3, changes in global mean cortical thickness were associated with depressive symptoms ($\beta = 0.053$, $P_{FDR} = 0.010$) and externalizing symptoms at T_2 ($\beta = 0.063$, $P_{FDR} = 0.002$), but not with internalizing symptoms ($\beta = 0.040$, $P_{FDR} = 0.051$). PGS-CRP was negatively associated with internalizing symptoms at T_2 ($\beta = -0.026$, $P_{FDR} = 0.043$) but positively associated with externalizing symptoms ($\beta = 0.033$, $P_{FDR} = 0.008$). No significant associations were found between PGS-CRP and depressive symptoms at T_2 ($\beta = -0.0005$, $P_{FDR} = 0.966$).

The indirect (mediation) effect of PGS-CRP on externalizing symptoms ($\beta = 0.002$, $P_{FDR} = 0.014$) and depression ($\beta = 0.002$, $P_{FDR} = 0.035$) through cortical thickness was significant, while the indirect effect on internalizing symptoms was not ($\beta = 0.001$, $P_{FDR} = 0.072$). Total effect estimates were significant between PGS-CRP and externalizing symptoms ($\beta = 0.035$, $P_{FDR} = 0.005$) but not internalizing symptoms ($\beta = -0.024$, $P_{FDR} = 0.051$) and depressive symptoms ($\beta = 0.001$, $P_{FDR} = 0.966$). Approximately 4% of the total effect of PGS-CRP on externalizing psychopathology was mediated through the change in cortical thickness. The detailed results are available in Supplementary Table 4.

**Fig. 3 | Path diagram illustrating the association between PGS-CRP and externalizing psychopathology, partially mediated by mean cortical thickness change.**

The pathway demonstrates that higher PGS-CRP was associated with accelerated cortical thinning, which, in turn, predicted increased externalizing symptoms. However, the mediation was partial (4% of total effect), as PGS-CRP also has a direct effect on externalizing psychopathology, indicating that the behavioral outcomes are not solely explained by cortical thinning. Statistical analysis was conducted using two-sided structural equation modeling. Indirect (mediation) effects were estimated using 1,000 bootstrap samples with bias-corrected 95% confidence intervals. All reported paths include standardized coefficients (beta/β) with exact P values, including FDR-corrected P values (P_{FDR}), and bootstrap confidence intervals are provided in Supplementary Table 4.

Biological annotation

We tested whether the regional effects of PGS-CRP on cortical thinning exhibited any correspondence with neurotransmitter receptor gradients. To explore this, we performed correlations between the effect map of PGS-CRP on cortical thinning and maps of various neurotransmitter receptor distributions. As shown in Fig. 4, our analysis revealed significant correlations between PGS-CRP effects and four specific neurotransmitter receptor gradients: serotonin (5HT₆, $r = -0.250$, $P_{uncorrected} = 0.010$, $P_{FDR} = 0.085$), gamma-aminobutyric acid type a receptor (GABAaR, $r = -0.274$, $P_{uncorrected} = 0.010$, $P_{FDR} = 0.085$), cannabinoid (CB₁, $r = -0.228$, $P_{uncorrected} = 0.020$, $P_{FDR} = 0.085$) and metabotropic glutamate receptor 5 (mGluR5, $r = -0.253$, $P_{uncorrected} = 0.020$, $P_{FDR} = 0.085$). Although these associations did not survive FDR correction, it highlighted that the regional effects of PGS-CRP on cortical thinning are possibly non-randomly distributed and align with neurotransmitter receptor gradients, emphasizing the role of immune-neurobiological pathways in cortical maturation and their potential contribution to psychopathology susceptibility. The full set of results is available in Supplementary Table 5.

Sensitivity analyses

To ensure the robustness of our findings, we conducted a sensitivity analysis by combining the European (EU) and non-European (non-EU) samples into a single full-sample analysis, rather than separating them and performing a meta-analysis. The results of the full-sample analysis were consistent with the meta-analytic approach, demonstrating similar directional effects across all primary outcomes. Notably, beyond the previously identified PGS-CRP by age interaction effect in the right entorhinal cortex, right insula cortex and right superior temporal gyrus, the combined sample revealed eight additional subregions that passed the statistical threshold of $P_{FDR} < 0.05$, reflecting the increased statistical power and precision afforded by the larger sample size (detailed results are provided in Supplementary Table 6). Furthermore, the association between PGS-CRP and externalizing psychopathology at baseline remains statistically significant (detailed results are provided in Supplementary Table 7). All associations between early-life infection and psychopathology remained statistically significant (detailed results are provided in Supplementary Table 8). Consistent with our primary

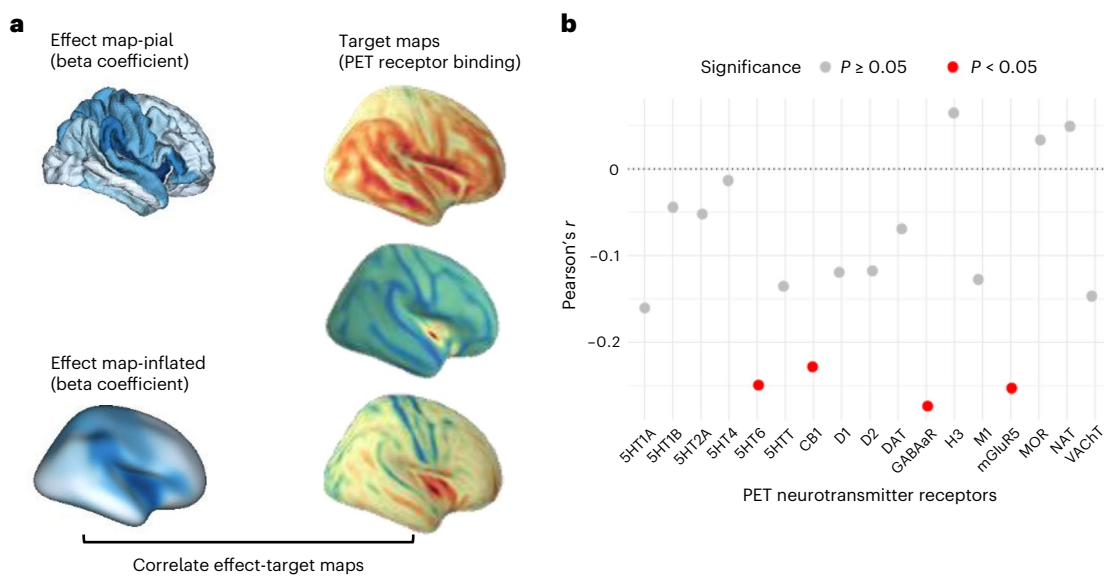


Fig. 4 | Regional association between PGS-CRP effects on cortical thinning and neurotransmitter receptor gradients. **a**, The left panel shows the regional age \times PGS-CRP interaction effects (standardized β coefficients) mapped onto the cortical surface. The right panel shows neurotransmitter receptor distributions based on PET receptor binding for corresponding regions. These neurotransmitter maps illustrate spatial receptor gradients; the colors are not indicative of specific data values or quantitative comparisons. **b**, The scatterplot depicts Pearson's correlation coefficients (r) between the regional PGS-CRP cortical-thinning effects and PET-derived neurotransmitter receptor gradients. X-axis labels correspond to serotonin receptors (5-HT1A, 5-HT1B, 5-HT2A, 5-HT4 and 5-HT6) and the serotonin transporter (5-HTT); the cannabinoid type-1

receptor (CB1); dopamine receptors (D1 and D2) and dopamine transporter (DAT); gamma-aminobutyric acid type-A receptor (GABA_AAA R); histamine H3 receptor (H3); muscarinic acetylcholine receptor M1 (M1) and vesicular acetylcholine transporter (VACHT); the norepinephrine transporter (NET); the metabotropic glutamate receptor 5 (mGluR5); and the mu-opioid receptor (MOR). Red points indicate significant correlations ($P_{\text{uncorrected}} < 0.05$). Statistical analysis used two-sided Pearson correlations, and spatial autocorrelation-preserving null models were used to generate significance thresholds. Exact correlation coefficients, P values and FDR-corrected values are provided in Supplementary Table 5.

findings, results remained unchanged when early-life infection was redefined using a stricter threshold (≥ 3 days of illness). Early-life infection shows no significant impact on cortical thickness (Supplementary Table 9), but independently increased the risk for psychopathology measurements (depression, internalizing and externalizing score) at the baseline (Supplementary Table 10). When youth-reported psychopathology (Brief Problem Monitor, BPM-Y at 6 months and 2 years; Supplementary Table 11) was examined, the association between early-life infection and externalizing symptoms replicated (FDR-corrected), consistent with caregiver reports. The association between PGS-CRP and externalizing psychopathology was in the same direction but did not reach significance, a pattern consistent with known phenomenon low to modest agreement between caregiver and youth informants⁴³ (Supplementary Table 11). To test whether our finding is sensitive to the selection of covariates, we re-estimated the models using the reduced model that included only ancestry-related covariates (genetic principal components), these effects remained, and eight additional subregions surpassed the FDR threshold ($P_{\text{FDR}} < 0.05$): right insula, right temporal pole, right entorhinal cortex, left entorhinal cortex, right pars opercularis, right superior temporal gyrus, left superior temporal gyrus and left pars opercularis (Supplementary Table 12). Similar to the original model, this reduced model also reproduced the association between PGS-CRP and externalizing psychopathology ($\beta = 0.206$, $P_{\text{FDR}} = 0.044$), while effects for internalizing and depression remained non-significant (Supplementary Table 13). These sensitivity analyses all yield consistent or stronger effects than the primary analyses, highlighting that the observed associations are robust and not dependent on the specific analytical strategy used.

Discussion

The primary goal of this study was to examine how genetic predisposition for systemic inflammation, as measured using a PGS-CRP,

influences adolescent neurodevelopment and the emergence of psychopathology, and explore its neurobiological mechanisms. Consistent with our initial hypotheses, higher genetic susceptibility to inflammation was associated with accelerated cortical thinning, particularly in medial temporal and insular regions, as well as increased externalizing psychopathology symptoms. Notably, we identified a significant indirect pathway wherein cortical thinning partially mediated the relationship between genetic predisposition to inflammation and both externalizing behaviors and depressive symptoms. Biological annotation analyses further suggested that the regions affected by PGS-CRP-related cortical thinning overlapped with neurotransmitter receptor systems enriched in serotonin, GABA, cannabinoid and glutamate signaling, highlighting the potential role of inflammation in disrupting these neurobiological pathways. These results underscore the importance of systemic inflammation as a key factor influencing neurodevelopmental trajectories during adolescence. Although the observed associations were modest in magnitude, this is consistent with the distributed and polygenic architecture of adolescent brain development and psychopathology. Small but replicable effects are common in large-scale imaging-genetic studies and are nonetheless informative for identifying biological pathways that may cumulatively shape developmental risk^{10,44,45}. Thus, even subtle inflammation-related differences in cortical maturation may have meaningful population-level implications for understanding the emergence of psychiatric vulnerability.

Accelerated cortical thinning during adolescence has been linked to a range of psychiatric outcomes. In schizophrenia, for example, progressive cortical thinning, particularly in the frontotemporal cortex, is associated with symptom severity and illness duration, from the first episode of psychosis through to the chronic stages of the disorder^{46,47}. Similarly, individuals with a high genetic risk for bipolar disorder show accelerated thinning and volume reduction in frontal regions, even

before the onset of the disorder⁴⁸. Extending these findings, our study suggests that genetic predisposition for inflammation, as measured by the PGS-CRP, may be a critical influencer of cortical developmental trajectories. This aligns with previous evidence linking cortical thinning during maturation to gene expression related to dendrites, dendritic spines and myelin, suggesting that shared molecular pathways may underlie both cortical development and psychiatric vulnerability^{7,49,50}. In our study, the brain regions most affected by accelerated thinning—such as the entorhinal cortex, superior temporal gyrus and insula—play key roles in integrating emotional and cognitive information. The superior temporal gyrus is crucial for auditory and language comprehension⁵¹, the insula detects relevant stimuli and coordinates neural resources for emotional and cognitive processing⁵², and the entorhinal cortex is essential for encoding and retrieving emotional memories⁵³. Moreover, the relationship between inflammation and cortical thinning appears to converge on molecular pathways involving complement component proteins such as C4A. These proteins, known for their role in synaptic pruning, have been linked to similar brain structural alterations (that is, insula and entorhinal cortex) and neurocognitive outcomes in both adolescent and adult samples^{54,55}. These findings are also consistent with neuroimaging research showing that inflammation disrupts neural circuits involved in emotional regulation and cognition²², thus supporting a potential neurobiological mechanism by which inflammation-related genetic risk factors influence psychiatric outcomes^{12,23,24}.

Building on these findings, the association between the PGS-CRP and externalizing psychopathology is notable. Externalizing behaviors, including aggression and rule-breaking, are often linked to difficulties in emotion regulation and impulse control. Our results suggest that systemic inflammation, driven by genetic factors, may impair the maturation of brain regions necessary for regulating behavior, increasing the risk for externalizing psychopathology. Importantly, these findings do not contradict the existing literature. While previous studies have primarily linked elevated inflammatory markers with fatigue, depression and stress-related disorders^{20,29,56,57}—commonly associated with energy-conserving ‘sickness behavior’—our results expand this understanding by implicating systemic inflammation in difficulties with decision-making and impulse regulation, which heighten the risk for externalizing psychopathology. Furthermore, we observed a significant increase in the association between the PGS-CRP and depression scores in the non-European ancestry sample (Supplementary Table 2), consistent with previous research. This discrepancy is likely attributable to our stringent statistical approach, which prioritizes robust and conservative estimates. In addition, it is important to note that the ABCD cohort primarily consists of adolescents without diagnosed depressive disorders, which may further attenuate associations between the PGS-CRP and depression scores.

Contrary to our hypotheses, early-life infection did not interact significantly with genetic risk to affect cortical thinning trajectories. However, early-life infection independently predicted increased risk for depressive and externalizing symptoms, reinforcing previous evidence that early immunological challenges can have lasting impacts on mood disorders³⁸. Our data support the ‘dual-hit’ hypothesis⁵⁸, where early environmental stressors, such as infections, interact with genetic predispositions to heighten the risk for psychopathology later in life. The impact of early immune activation on neurodevelopment may sensitize the brain immune cell microglia (microglia priming)⁵⁹ to subsequent inflammatory stimuli, further disrupting normal synaptic pruning or other maturation processes. The absence of a significant interaction with genetic predisposition could reflect limitations in statistical power or distinct biological pathways through which early-life infections and genetic risk independently contribute to psychopathology. In addition, our reliance on parental reporting of early-life infections introduces the possibility of recall bias and lacks detailed information regarding infection source, severity and duration. Future

Table 2 | Basic demographic¹, exposure and outcome variables in full analytical sample, stratified by ancestry and year

EU sample (sample 1)	Year 0 (n=6,336)	Year 2 (n=4,617)
Mean cortical thickness (mean (s.d.) ²)	2.74 (0.08)	2.70 (0.08)
Depression (mean (s.d.))	53.60 (5.66)	53.94 (6.02)
Internalizing (mean (s.d.))	48.70 (10.45)	48.30 (10.33)
Externalizing (mean (s.d.))	45.42 (10.01)	44.47 (9.65)
Polygenic score for CRP (mean (s.d.))	-0.18 (0.93)	-0.18 (0.93)
Age (years)	9.92 (0.63)	11.96 (0.65)
Sex at birth, female (%)	2,982 (47.1%)	2,080 (45.1%)
Body mass index (mean (s.d.))	17.92 (3.31)	19.69 (4.01)
Non-EU sample (sample 2)	Year 0 (n=4,878)	Year 2 (n=3,206)
Mean cortical thickness (mean (s.d.))	2.70 (0.08)	2.66 (0.08)
Depression (mean (s.d.))	53.61 (5.80)	53.55 (5.83)
Internalizing (mean (s.d.))	48.19 (10.91)	46.96 (10.76)
Externalizing (mean (s.d.))	46.26 (10.74)	44.81 (10.18)
Polygenic score for CRP (mean (s.d.))	0.25 (1.04)	0.24 (1.03)
Age (years)	9.90 (0.62)	11.94 (0.66)
Sex at birth, female (%)	2,347 (48.1%)	1,511 (47.1%)
Body mass index (mean (s.d.))	19.78 (4.46)	21.66 (4.80)
Full meta-analysis sample	Year 0 (n=11,214)	Year 2 (n=7,823)
Mean cortical thickness (mean (s.d.))	2.72 (0.08)	2.69 (0.08)
Depression (mean (s.d.))	53.60 (5.72)	53.78 (5.95)
Internalizing (mean (s.d.))	48.48 (10.66)	47.75 (10.53)
Externalizing (mean (s.d.))	45.77 (10.34)	44.63 (9.87)
Polygenic score for CRP (mean (s.d.))	0.00 (1.00)	-0.01 (1.00)
Early-life infection, yes (%)	1,710 (16.7%)	1,218 (16.9%)
Age (years)	9.91 (0.63)	11.95 (0.65)
Sex at birth, female (%)	5,329 (47.5%)	3,591 (45.9%)
Body mass index (mean (s.d.))	18.73 (3.96)	20.49 (4.45)

¹Owing to page limitations, detailed socioeconomic variables (race/ethnicity, parental education and household income) are presented in Supplementary Table 14. ²s.d., standard deviation.

studies should incorporate more objective and detailed measures of early-life infection—including clinical diagnoses, infection severity, duration and specific pathogens—to improve our understanding of how these factors interact with genetic inflammation susceptibility to influence neurodevelopmental trajectories.

The biological annotations provide deeper insights into the neurobiological mechanisms at play. Specifically, we found a significant overlap between regions of cortical thinning associated with the PGS-CRP and neurotransmitter receptor gradients for serotonin, GABA, cannabinoid and glutamate signaling. This aligns with decades of animal research showing that inflammation critically modifies neurotransmitter systems, thereby increasing the risk of psychiatric disorders^{58,60}. Notably, while inflammation and disruptions in serotonin and glutamate signaling have been extensively studied in relation to ‘sickness behaviors’ such as fatigue and depression^{61–64}, our findings extend this perspective. Our findings, while preliminary, indicate potential neurochemical pathways through which genetic predisposition for inflammation may alter cortical development, contributing to externalizing psychopathology, which includes deficits in emotion regulation, poor impulse control and impaired decision-making.

Our findings have important clinical implications, highlighting genetic predispositions to systemic inflammation as key factors in adolescent brain development and psychopathology, opening avenues for early intervention. Targeting inflammation in at-risk individuals could help prevent psychopathology through anti-inflammatory treatments or lifestyle interventions such as exercise and dietary changes. Early identification of children with higher genetic liability for systemic inflammation may also help clinicians identify those at higher risk for neurodevelopmental disorders or psychiatric symptoms. However, several limitations of this study must be acknowledged. While we used a polygenic score for CRP to assess genetic predisposition for inflammation, it explains only a fraction of the variance in plasma CRP levels, limiting its comprehensiveness. In addition, the CRP genome-wide association study (GWAS) used to derive the polygenic score was based on data from the UK Biobank, a predominantly European adult cohort. While gene expression for phenotypes may change over time⁶⁵, research has shown that the genetic architecture of brain phenotypes is generalizable across age⁶⁶ and polygenic predictions for psychopathology can be effective even when the training data comes from an adult population (such as UK Biobank)⁶⁷. It is true that there are known difficulties in translating findings from one ancestry to another⁶⁸. We did choose polygenic scoring methods that attempt to overcome these difficulties⁶⁹, and the convergent findings across ancestry grouping give us confidence in our results. Future research should work to include diverse populations at all levels of genetics research and should work to further validate these findings across multiple ancestries. Our findings were robust when early-life infection was redefined using a stricter threshold (≥ 3 days of illness), although we acknowledge that reliance on parental recall remains a limitation. Moreover, the lack of longitudinal measures of circulating CRP may have restricted our ability to capture the dynamic relationship between systemic inflammation and neurodevelopment. Future research should explore the interplay between genetic risk for inflammation and environmental pro-inflammatory factors—such as early-life adversity, viral infections or diet—to better understand their contributions to neurodevelopmental trajectories.

Conclusion

Our findings revealed genetic predisposition to systemic inflammation, as quantified by a polygenic score for CRP, as a critical factor influencing adolescent neurodevelopmental trajectories and psychopathology risk. Specifically, elevated genetic susceptibility to inflammation was robustly associated with accelerated cortical thinning, particularly in regions vital for emotional and cognitive processing, and increased externalizing behavioral symptoms. Importantly, we identified cortical thinning as a partial mediator of the link between inflammation-related genetic risk and psychopathology, highlighting a tangible neurodevelopmental pathway through which genetic predispositions can manifest in behavioral dysfunction. While early-life infections independently heightened psychopathological risks, their interaction with genetic predisposition requires further nuanced investigation with detailed clinical data. In addition, exploratory biological annotation suggested that disruptions of neurotransmitter receptor systems (serotonin, GABA, cannabinoid and glutamate) may underpin these inflammation-linked cortical changes. Collectively, these findings highlight systemic inflammation as a potential target for early identification and preventive interventions in youth at elevated risk, offering critical insights into the complex neuroimmune mechanisms that contribute to mental health disorders emerging during adolescence. Future studies should build upon these results by integrating detailed longitudinal measures of inflammation, environmental exposures and precise mechanistic investigations to deepen our understanding of these critical developmental pathways.

Methods

Ethics statement

The ABCD Study obtained institutional review board approval at each participating site, and written informed consent from parents/guardians and assent from children were collected by ABCD investigators. The present study involved secondary analysis of fully de-identified data available through the NIMH Data Archive and was therefore determined not to involve human subjects research and did not require additional ethical review.

Study design and population

This longitudinal cohort study utilized data from the ABCD Study, an ongoing large-scale sample of 11,868 youth aged 9–10 years at baseline; 47.1% were assigned female at birth. Families received monetary compensation for participation, consistent with ABCD Study protocols. Recruitment was conducted primarily through public and private elementary schools using a probability sampling approach stratified by age, sex, race/ethnicity, socioeconomic status and urbanicity, with targeted oversampling of racial/ethnic groups historically underrepresented in research (for example, Black, Hispanic and rural youth) to better reflect the US population⁷⁰. The participating schools were drawn from each site's catchment area, collectively encompassing ~20% of the US population of 9–10-year-olds. Approximately 9.6% of the contacted families enrolled, yielding a cohort broadly representative of the sociodemographic composition of US children⁷⁰. Enrollment demographics were monitored throughout recruitment, and later school samples were dynamically adjusted to correct deviations from target demographics⁷⁰. Approximately half of the sample was enriched for children with early indicators of externalizing or internalizing symptoms to ensure sufficient power for studying developmental risk trajectories⁷¹. At baseline (T_0 , $n = 11,214$), 99% of the participants completed the T1-weighted structural MRI. At the 2-year follow-up (T_2 , $n = 7,823$), approximately 70% of the baseline cohort have finished the second MRI scan and available in ABCD data release 5.1. Basic demographic characteristics, exposure and outcome variables for baseline, year 2 and ancestry-stratified samples are shown in Table 2. Owing to page limitations, additional socioeconomic characteristics (race/ethnicity, parental education and household income) for the full sample and genetic ancestry-stratified samples are presented in Supplementary Table 14. Demographic, clinical and structural MRI data were obtained from the National Institutes of Mental Health Data Archive (NDA). Full recruitment details and neuroimaging acquisition are available in previous publications^{70,71}.

Exclusion criteria for the ABCD Study included non-fluency in English, not having a guardian fluent in English or Spanish, major medical or neurological conditions, gestational age below 28 weeks or birthweight under 1,200 grams, contraindications for MRI scanning, a history of traumatic brain injury, current diagnosis of schizophrenia, moderate to severe autism spectrum disorder, intellectual disability or alcohol/substance use disorder.

This report was based on data from the ABCD 5.1 data release. The data analyzed were collected between September 1, 2016, and February 15, 2021. Of the 11,868 participants in the original cohort, 140 had missing baseline (year 0) MRI data, 476 had missing PGS-CRP data, 36 were screened at a site that dropped out of the ABCD Study, and 2 had missing genetic ancestry data and were excluded, yielding a final analytic sample of 11,214. Participants were stratified by genetically inferred continental-ancestry clusters (European ($n = 6,336$) versus non-European ($n = 4,878$)) based on genetic ancestry score thresholds (≥ 0.8 versus < 0.8). Within each ancestry group, follow-up data were available for the majority: 4,588 European ancestry and 3,158 non-European ancestry youth completed both baseline and year 2 assessments, while others did not complete year 2 primarily owing to attrition or incomplete visits. A flow diagram (Fig. 1) summarizes the number of participants at each stage of inclusion, exclusion and

follow-up. In addition, missingness across exposures (PGS-CRP, early-life infection), outcomes (cortical thickness, psychopathology) and covariates is summarized in Supplementary Table 15. Attrition between baseline and year 2 is detailed in Supplementary Table 16. This report follows the Strengthening the Reporting of Observational Studies in Epidemiology (STROBE) reporting guidelines.

Exposure variables

Polygenic score calculation. *Genome-wide association data.* The primary exposure variable for this report was the PGS-CRP, which provides a quantitative instrument of an individual's genetic propensity for elevated systemic inflammation. We generated the PGS-CRP using summary statistics from the UK Biobank participants ($N = 427,367$, European descent) and the Cohorts for Heart and Aging Research in Genomic Epidemiology (CHARGE) Consortium (total $N = 575,531$ European descent)³⁶ accessed from the GWAS Catalog⁷² under accession code **GCST90029070** (<https://www.ebi.ac.uk/gwas/studies/GCST90029070>). Summary statistics were cleaned and aligned to genome build GRCh38 using the function `cleansumstats`⁷³.

ABCD genetic data. Genetic data was collected using blood or saliva samples from participants of the ABCD Study⁷⁴. A total of 656,247 genomic markers were measured using Smokescreen array⁷⁵. To increase the amount of overlap in genetic variants between the ABCD sample and the CRP GWAS, we imputed the markers from our Smokescreen array using the TOPMED imputation server⁷⁶. These imputed variants were fractional dosages and were converted to an integer number of alleles using a best guess threshold of 0.9 resulting in over 280 million imputed variants aligned to genome build GRCh38. After imputation target genetic data was restricted to only autosomal variants with a minor allele frequency of 1% (0.01) or greater leaving just under 11 million single nucleotide polymorphisms (SNPs) in the target data. Genetic continental ancestry was estimated using SNPweights⁷⁷ and external genomic reference panels for African, East Asian, European⁷⁸, and Indigenous North and South American⁷⁹ ancestry populations. Individuals with inferred genetic ancestry at least 80% (0.8) consistent with the European ancestry reference panels were considered European ancestry (EU sample, $N = 6,605$ at baseline and $N = 5,992$ at follow-up), and all others were grouped into the non-European ancestry sample (non-EU sample, $N = 4,500$ at baseline and $N = 3,750$ at follow-up).

Polygenic score computation. Best practices for imputing polygenic scores in the ABCD are based on the results of a previous analysis that found that the Bayesian polygenic scoring method, PRScs⁸⁰, maximized variance explained while maintaining a manageable computational load and improving or maintaining performance across ancestry compared with other Bayesian and pruning and thresholding methods⁶⁹. Posterior effect sizes were generated using PRScs using 10,000 Markov Chain Monte Carlo iterations and 5,000 burnin interactions. All other parameters were left at their default. Linkage disequilibrium reference panels required for this analysis were based on data from 1000 Genomes Phase 3 and matched the ancestry of the summary statistics. Posterior effect sizes were applied to ABCD target data converted to polygenic scores using PLINK 2.0 (ref. 81).

Early-life infection

The secondary exposure variable was early-life infection, operationalized as a binary indicator based on parental reports of infant illness. Specifically, parents were asked: 'How many days in the first 12 months of life did your child have any severe infections?' Owing to the lack of detailed diagnostic information (for example, infection type, severity or duration), we applied a binary coding approach: responses indicating no reported sick days were coded as 0 (no severe early-life infection), and those reporting one or more days of illness were coded as 1 (presence of severe early-life infection). Although limited in clinical

detail, this measure provides a proxy for early-life infection as a biological stressor.

Outcome variables

The primary outcomes of interest were MRI indices of cortical thickness and measures of psychopathology. MRI acquisition and processing adhered to the standardized protocols of the ABCD Study^{71,82}. Imaging data were acquired on three types of 3T scanner—Siemens Prisma/Prisma Fit, GE MR750 and Philips Achieva dStream/Ingenia. T1-weighted images were corrected for gradient nonlinearity distortions using scanner-specific transformations, and cortical reconstruction and volumetric segmentation were performed using FreeSurfer v7.1.1, which includes procedures addressing head motion, distortion and intensity inhomogeneity⁸². Cortical thickness estimates were derived for 34 parcellations per hemisphere according to the Desikan–Killiany atlas⁸³. All imaging data were previously collected and preprocessed by the ABCD Data Analysis, Informatics, and Resource Center (DAIRC), which performed both automated and manual quality control before data release. No new MRI data were generated for the present analyses.

Psychopathology was assessed using the depression, internalizing and externalizing symptom scales from the parent-reported Child Behavior Checklist (CBCL). The CBCL is a well-validated and widely used tool for evaluating youth mental health, known for its high reliability and internal consistency⁸⁴. It consists of eight syndrome scales (anxious, depressed, somatic complaints, social problems, thought problems, attention problems, rule-breaking behavior and aggressive behavior) that load into two broad categories: internalizing and externalizing problems⁸⁵. The internalizing and externalizing scores from CBCL are commonly used for identifying broad patterns of emotional and behavioral problems⁸⁵. Depression was examined as a distinct outcome owing to its connection inflammatory markers in the literature and its central role in mental health disorders⁵⁷. The continuous estimation of depression was derived from CBCL DSM-5 oriented affective problem scale, developed in the 2001 revision of the CBCL. Parents rated the presence of specific child behaviors over the past 6 months using a scale of 0 ('not true'), 1 ('somewhat or sometimes true') or 2 ('very true or often true'), with higher scores representing more notable psychopathology.

Covariates

Sex at birth, body mass index, self-reported race/ethnicity, parental education, household income and the first ten principal components of genetic ancestry (to account for population stratification) were included as fixed-effect covariates in analyses. These covariates have been previously reported to be associated with systemic inflammation and mental health outcomes. Parental education and household income were reported by the guardian and are key indicators of socio-economic status, known to be associated with neurodevelopmental trajectories and psychopathology^{86,87}. The ten principal components of genetic ancestry were derived from the ABCD genetic data to account for population stratification across diverse ancestral backgrounds, thereby minimizing spurious associations unrelated to the exposure and outcomes of interest. The detailed methodology for computing these genetic principal components has been previously published⁸⁸. Together, these covariates were included to control for confounds and to help isolate the unbiased effects of the primary exposure variables on the outcomes of interest.

In addition, individual, family and study site were included as random-effect covariates in the analyses to account for nesting of the data with respect to these variables. Individual random effects account for nesting of participants' repeated measurement occasions (two visits). Many ABCD Study participants come from families with siblings also in the study (9,420 families); hence, family random effects account for nesting of data within families. Finally, there are 21 data

collection sites in the ABCD Study, and site random intercepts account for nesting at this level.

Statistical analyses

Participants were stratified by imputed genetic ancestry into two groups to account for population stratification: sample 1, individuals of European ancestry (EU sample, $N=6,605$ at baseline and $N=5,992$ at follow-up), and sample 2, individuals of non-European ancestry (non-EU sample, $N=4,500$ at baseline and $N=3,750$ at follow-up; see 'ABCD genetic data' for further details). This stratification was conducted to mitigate bias arising from population stratification, a phenomenon where differences in allele frequencies across ancestral groups reflect demographic history rather than trait-specific associations⁶⁸ and to help account for known difference in polygenic score performance when translating across ancestries⁶⁸. Given that genetic variants contributing to polygenic scores can vary in frequency and effect size between populations, stratification ensures that the polygenic scores reliably capture ancestry-specific genetic risk, thereby enhancing the validity and generalizability of the findings⁶⁸.

A meta-analysis was conducted to integrate findings across participants of European and non-European ancestry samples. This approach was chosen to synthesize results from diverse genetic backgrounds, enhancing the generalizability of our findings and providing a robust assessment of the genetic influences on neurodevelopmental outcomes across different populations. Statistical significance was evaluated using an FDR threshold of $P<0.05$ of meta-analysis results.

Linear mixed-effects (LME) models were used to examine whether genetic predisposition to systemic inflammation, as indexed by the PGS-CRP, was associated with cortical thickness trajectories and psychopathology risk during adolescence (primary hypothesis), and whether this association was moderated by early-life infection (secondary hypothesis). The model included a three-way interaction between PGS-CRP, age and early-life infection, with age modeled continuously to capture longitudinal change from baseline (T_0) to follow-up (T_2).

The model was specified as

$$\begin{aligned} \text{Outcomes}_{ijk} = & \beta_0 + \beta_1 (\text{Age}_{ijk}) + \beta_2 (\text{PGS} - \text{CRP}_i) + \beta_3 (\text{Age}_{ijk} \times \text{PGS} - \text{CRP}_i) \\ & + \beta_4 (\text{EarlyLifeInfection}_i) + \beta_5 (\text{Age}_{ijk} \times \text{EarlyLifeInfection}_i) \\ & + \beta_6 (\text{PGS} - \text{CRP}_i \times \text{EarlyLifeInfection}_i) \\ & + \beta_7 (\text{Age}_{ijk} \times \text{PGS} - \text{CRP}_i \times \text{EarlyLifeInfection}_i) \\ & + X_{ijk}\beta + u_i + u_j + w_k + \varepsilon_{ijk} \end{aligned}$$

where i, j and k index individuals, families and study sites, respectively. X includes fixed-effect covariates: sex, body mass index, race, parental education, household income and the first ten principal components of genetic ancestry. The random effects include individual ID (u_i), family ID (u_j) and study site (w_k). The ε_{ijk} represents the residual error. All continuous predictors were standardized before analysis.

Mediation analyses

We implemented structural equation models (SEMs) to examine whether changes in cortical thickness mediate the association between PGS-CRP and psychopathology. SEMs included depressive, internalizing and externalizing symptoms at 2-year follow-up as outcome variables; each was regressed on changes in global mean cortical thickness ($T_2 - T_0$), PGS-CRP, age at T_2 , sex, baseline cortical thickness and baseline psychopathology symptoms. Global mean cortical thickness change was included as a mediator of the PGS-CRP to psychopathology relationship. Although primary analyses tested regional thickness associations, global cortical thinning was used in the mediation models to capture a unified index of brain maturation. This is supported by cortical thinning during adolescence as a global coordinated process

reflecting normative neurodevelopment. Using global thickness change provides a developmentally meaningful and statistically efficient summary of individual differences in cortical maturation. One thousand bootstrap samples were used to obtain robust estimates and confidence intervals for direct and indirect effects. Model fit was evaluated using the comparative fit index, Tucker–Lewis index and standardized root mean square residual.

Biological annotation

To explore the potential biological mechanisms underlying the effects of PGS-CRP on cortical thinning in adolescents, we conducted a neurobiological annotation analysis using the Neuromaps toolbox⁸⁹. In this framework, 'annotation' refers to testing whether the spatial pattern of cortical effects associated with PGS-CRP aligns with known maps of neurotransmitter receptor density. We compared our cortical effect maps with standardized PET-derived receptor distribution maps spanning 17 receptors and transporters across 9 neurotransmitter systems. These include serotonin (5-HT_{1A}⁹⁰, 5-HT_{1B}⁹⁰, 5-HT_{2A}⁹¹, 5-HT_{2B}⁹¹, 5-HT₆⁹² and 5-HT₇⁹¹), cannabinoid (CB₁⁹³), dopamine (D₁⁹⁴, D₂⁹⁵ and DAT⁹⁶), gamma-aminobutyric acid type a receptor (GABA_A⁹⁷), histamine (H₃⁹⁸), norepinephrine (NET⁹⁹), acetylcholine (M₁¹⁰⁰ and VACHT¹⁰¹), glutamate (mGluR₅¹⁰²) and opioid (MOR¹⁰³). To rigorously assess spatial correspondence, we applied spatial autocorrelation-preserving permutation tests, termed spatial null model^{89,104}. This approach generates null distributions that maintain the intrinsic spatial smoothness of cortical maps, allowing robust statistical evaluation of whether observed receptor–cortical thinning associations exceed chance. This procedure provides insights into whether genetic liability to inflammation influences cortical regions that overlap with specific neurotransmitter systems, thereby offering a molecular-level interpretation of observed neuroimaging effects.

Reporting summary

Further information on research design is available in the Nature Portfolio Reporting Summary linked to this article.

Data availability

This study used data from the Adolescent Brain Cognitive Development (ABCD) Study, curated release 5.1. These data are publicly available through the National Institute of Mental Health Data Archive (NDA) under the ABCD collection (<https://nda.nih.gov/abcd>). Access requires completion of the NDA Data Use Certification.

Code availability

No custom algorithms were developed for this study. Analyses were performed using publicly available software, including PLINK 2.0 and PRS-CS for genetic analyses; FreeSurfer v7.1.1 for neuroimaging processing; and R (version 4.4.1) with the packages nlme (v3.1-168), metafor (v4.8-0) and lavaan (v0.6-19) for statistical modeling and mediation analyses. Neurobiological annotation was conducted using the Neuromaps toolbox. All software used in this study is freely accessible.

References

1. Fuhrmann, D., Madsen, K. S., Johansen, L. B., Baaré, W. F. C. & Kievit, R. A. The midpoint of cortical thinning between late childhood and early adulthood differs between individuals and brain regions: evidence from longitudinal modelling in a 12-wave neuroimaging sample. *NeuroImage* **261**, 119507 (2022).
2. Fjell, A. M. et al. Development and aging of cortical thickness correspond to genetic organization patterns. *Proc. Natl Acad. Sci. USA* **112**, 15462–15467 (2015).
3. Amlie, I. K. et al. Organizing principles of human cortical development—thickness and area from 4 to 30 years: insights from comparative primate neuroanatomy. *Cereb. Cortex* **26**, 257–267 (2016).

4. Paus, T., Keshavan, M. & Giedd, J. N. Why do many psychiatric disorders emerge during adolescence? *Nat. Rev. Neurosci.* **9**, 947–957 (2008).
5. Huttenlocher, P. R. & Dabholkar, A. S. Regional differences in synaptogenesis in human cerebral cortex. *J. Comp. Neurol.* **387**, 167–178 (1997).
6. Huttenlocher, P. R. Synaptic density in human frontal cortex—developmental changes and effects of aging. *Brain Res.* **163**, 195–205 (1979).
7. Parker, N. et al. Assessment of neurobiological mechanisms of cortical thinning during childhood and adolescence and their implications for psychiatric disorders. *JAMA Psychiatry* **77**, 1127–1136 (2020).
8. Petanjek, Z. et al. Extraordinary neoteny of synaptic spines in the human prefrontal cortex. *Proc. Natl Acad. Sci. USA* **108**, 13281–13286 (2011).
9. Tamnes, C. K. et al. Development of the cerebral cortex across adolescence: a multisample study of inter-related longitudinal changes in cortical volume, surface area, and thickness. *J. Neurosci.* **37**, 3402–3412 (2017).
10. Bethlehem, R. A. I. et al. Brain charts for the human lifespan. *Nature* **604**, 525–533 (2022).
11. Zhao, Q. et al. The ABCD Study: brain heterogeneity in intelligence during a neurodevelopmental transition stage. *Cereb. Cortex* **32**, 3098–3109 (2022).
12. Kuang, N. et al. Neurodevelopmental risk and adaptation as a model for comorbidity among internalizing and externalizing disorders: genomics and cell-specific expression enriched morphometric study. *BMC Med.* **21**, 291 (2023).
13. Romer, A. L., Ren, B. & Pizzagalli, D. A. Brain structure relations with psychopathology trajectories in the ABCD Study. *J. Am. Acad. Child Adolesc. Psychiatry* **62**, 895–907 (2023).
14. Bos, M. G. N., Peters, S., van de Kamp, F. C., Crone, E. A. & Tamnes, C. K. Emerging depression in adolescence coincides with accelerated frontal cortical thinning. *J. Child Psychol. Psychiatry* **59**, 994–1002 (2018).
15. Yu, G. et al. Common and disorder-specific cortical thickness alterations in internalizing, externalizing and thought disorders during early adolescence: an Adolescent Brain and Cognitive Development study. *J. Psychiatry Neurosci.* **48**, E345–E356 (2023).
16. Stevens, B. et al. The classical complement cascade mediates CNS synapse elimination. *Cell* **131**, 1164–1178 (2007).
17. Bohlson, S. S. & Tenner, A. J. Complement in the brain: contributions to neuroprotection, neuronal plasticity, and neuroinflammation. *Annu. Rev. Immunol.* <https://doi.org/10.1146/annurev-immunol-101921-035639> (2023).
18. Vidal-Pineiro, D. et al. Cellular correlates of cortical thinning throughout the lifespan. *Sci. Rep.* **10**, 21803 (2020).
19. Vainchtein, I. D. et al. Astrocyte-derived interleukin-33 promotes microglial synapse engulfment and neural circuit development. *Science* **359**, 1269–1273 (2018).
20. Miller, A. H. & Raison, C. L. The role of inflammation in depression: from evolutionary imperative to modern treatment target. *Nat. Rev. Immunol.* **16**, 22–34 (2016).
21. Riester, K. et al. In vivo characterization of functional states of cortical microglia during peripheral inflammation. *Brain Behav. Immun.* **87**, 243–255 (2020).
22. Goldsmith, D. R., Bekhbat, M., Mehta, N. D. & Felger, J. C. Inflammation-related functional and structural dysconnectivity as a pathway to psychopathology. *Biol. Psychiatry* **93**, 405–418 (2023).
23. Barker, E. D. et al. Inflammation-related epigenetic risk and child and adolescent mental health: a prospective study from pregnancy to middle adolescence. *Dev. Psychopathol.* **30**, 1145–1156 (2018).
24. Jones, H. J. et al. Association of genetic risk for rheumatoid arthritis with cognitive and psychiatric phenotypes across childhood and adolescence. *JAMA Netw. Open* **2**, e196118 (2019).
25. Hurlmann, J., Thorbecke, G. J. & Hochwald, G. M. The liver as the site of C-reactive protein formation. *J. Exp. Med.* **123**, 365–378 (1966).
26. Rhodes, B., Furnrohr, B. G. & Vyse, T. J. C-reactive protein in rheumatology: biology and genetics. *Nat. Rev. Rheumatol.* **7**, 282–289 (2011).
27. Baumann, H. & Gauldie, J. The acute phase response. *Immunol. Today* **15**, 74–80 (1994).
28. Felger, J. C. et al. What does plasma CRP tell us about peripheral and central inflammation in depression? *Mol. Psychiatry* **25**, 1301–1311 (2020).
29. Ironside, M. et al. Inflammation and depressive phenotypes: evidence from medical records from over 12 000 patients and brain morphology. *Psychol. Med.* **50**, 2790–2798 (2020).
30. Zheng, H. et al. C-Reactive protein and the kynurenic acid to quinolinic acid ratio are independently associated with white matter integrity in major depressive disorder. *Brain Behav. Immun.* **105**, 180–189 (2022).
31. Pitharouli, M. C. et al. Elevated C-reactive protein in patients with depression, independent of genetic, health, and psychosocial factors: results from the UK Biobank. *Am. J. Psychiatry* **178**, 522–529 (2021).
32. Osimo, E. F., Baxter, L. J., Lewis, G., Jones, P. B. & Khandaker, G. M. Prevalence of low-grade inflammation in depression: a systematic review and meta-analysis of CRP levels. *Psychol. Med.* **49**, 1958–1970 (2019).
33. Fernandes, B. S. et al. C-reactive protein concentrations across the mood spectrum in bipolar disorder: a systematic review and meta-analysis. *Lancet Psychiatry* **3**, 1147–1156 (2016).
34. Fernandes, B. S. et al. C-reactive protein is increased in schizophrenia but is not altered by antipsychotics: meta-analysis and implications. *Mol. Psychiatry* **21**, 554–564 (2016).
35. Figueroa-Hall, L. K. et al. Psychiatric symptoms are not associated with circulating CRP concentrations after controlling for medical, social, and demographic factors. *Transl. Psychiatry* **12**, 279 (2022).
36. Said, S. et al. Genetic analysis of over half a million people characterises C-reactive protein loci. *Nat. Commun.* **13**, 2198 (2022).
37. Mac Giollabhui, N. et al. Role of inflammation in depressive and anxiety disorders, affect, and cognition: genetic and non-genetic findings in the lifelines cohort study. *Transl. Psychiatry* **15**, 164 (2025).
38. Benros, M. E. et al. Autoimmune diseases and severe infections as risk factors for mood disorders: a nationwide study. *JAMA Psychiatry* **70**, 812–820 (2013).
39. Köhler-Forsberg, O. et al. A nationwide study in Denmark of the association between treated infections and the subsequent risk of treated mental disorders in children and adolescents. *JAMA Psychiatry* **76**, 271–279 (2019).
40. Bilbo, S. D. & Schwarz, J. M. Early-life programming of later-life brain and behavior: a critical role for the immune system. *Front. Behav. Neurosci.* **3**, 14 (2009).
41. Bland, S. T. et al. Enduring consequences of early-life infection on glial and neural cell genesis within cognitive regions of the brain. *Brain Behav. Immun.* **24**, 329–338 (2010).
42. Lavebratt, C. et al. Early exposure to antibiotic drugs and risk for psychiatric disorders: a population-based study. *Transl. Psychiatry* **9**, 317 (2019).
43. De Los Reyes, A. et al. The validity of the multi-informant approach to assessing child and adolescent mental health. *Psychol. Bull.* **141**, 858–900 (2015).

44. Marek, S. et al. Reproducible brain-wide association studies require thousands of individuals. *Nature* **603**, 654–660 (2022).

45. Dick, A. S. et al. Meaningful associations in the Adolescent Brain Cognitive Development Study. *NeuroImage* **239**, 118262 (2021).

46. Youjin, Z. et al. Cortical thickness abnormalities at different stages of the illness course in schizophrenia. *JAMA Psychiatry* **79**, 560–570 (2022).

47. Erp, T. V. V. et al. Cortical brain abnormalities in 4474 individuals with schizophrenia and 5098 control subjects via the enhancing neuro imaging genetics through meta analysis (ENIGMA) consortium. *Biol. Psychiatry* **84**, 644–654 (2018).

48. Roberts, G. et al. Accelerated cortical thinning and volume reduction over time in young people at high genetic risk for bipolar disorder. *Psychol. Med.* **52**, 1344–1355 (2020).

49. Baselmans, B. et al. The genetic and neural substrates of externalizing behavior. *Biol. Psychiatry Glob. Open Sci.* **2**, 389–399 (2022).

50. Tandberg, A. D. et al. Individual differences in internalizing symptoms in late childhood: a variance decomposition into cortical thickness, genetic and environmental differences. *Dev Sci.* <https://doi.org/10.1111/desc.13537> (2024).

51. Bhaya-Grossman, I. & Chang, E. F. Speech computations of the human superior temporal gyrus. *Annu. Rev. Psychol.* **73**, 79–102 (2022).

52. Uddin, L. Q. Salience processing and insular cortical function and dysfunction. *Nat. Rev. Neurosci.* **16**, 55–61 (2015).

53. Kristina, D., Ferris, C. & Hamann, S. Neural correlates of successful emotional episodic encoding and retrieval: an SDM meta-analysis of neuroimaging studies. *Neuropsychologia* <https://doi.org/10.1016/j.neuropsychologia.2020.107495> (2020).

54. Hernandez, L. M. et al. Multi-ancestry phenoome-wide association of complement component 4 variation with psychiatric and brain phenotypes in youth. *Genome Biol.* **24**, 42 (2023).

55. O'Connell, K. S. et al. Association between complement component 4A expression, cognitive performance and brain imaging measures in UK Biobank. *Psychol. Med.* **52**, 1–11 (2021).

56. Zeng, Y. et al. Inflammatory biomarkers and risk of psychiatric disorders. *JAMA Psychiatry* <https://doi.org/10.1001/jamapsychiatry.2024.2185> (2024).

57. Dantzer, R., O'Connor, J. C., Freund, G. G., Johnson, R. W. & Kelley, K. W. From inflammation to sickness and depression: when the immune system subjugates the brain. *Nat. Rev. Neurosci.* **9**, 46–56 (2008).

58. Guerrin, C. G. J., Doorduin, J., Sommer, I. E. & de Vries, E. F. J. The dual hit hypothesis of schizophrenia: evidence from animal models. *Neurosci. Biobehav. Rev.* **131**, 1150–1168 (2021).

59. Neher, J. J. & Cunningham, C. Priming microglia for innate immune memory in the brain. *Trends Immunol.* **40**, 358–374 (2019).

60. Howes, O. D., McCutcheon, R., Owen, M. J. & Murray, R. M. The role of genes, stress, and dopamine in the development of schizophrenia. *Biol. Psychiatry* **81**, 9–20 (2017).

61. Haroon, E. et al. Increased inflammation and brain glutamate define a subtype of depression with decreased regional homogeneity, impaired network integrity, and anhedonia. *Transl. Psychiatry* **8**, 189 (2018).

62. Haroon, E., Miller, A. H. & Sanacora, G. Inflammation, glutamate, and glia: a trio of trouble in mood disorders. *Neuropsychopharmacology* **42**, 193–215 (2017).

63. Felger, J. C. et al. Inflammation is associated with decreased functional connectivity within corticostratial reward circuitry in depression. *Mol. Psychiatry* **21**, 1358–1365 (2016).

64. Felger, J. C. & Treadway, M. T. Inflammation effects on motivation and motor activity: role of dopamine. *Neuropsychopharmacology* **42**, 216–241 (2017).

65. Glass, D. et al. Gene expression changes with age in skin, adipose tissue, blood and brain. *Genome Biol.* **14**, R75 (2013).

66. Makowski, C. et al. Discovery of genomic loci of the human cerebral cortex using genetically informed brain atlases. *Science* **375**, 522–528 (2022).

67. Jansen, A. G. et al. The predictive capacity of psychiatric and psychological polygenic risk scores for distinguishing cases in a child and adolescent psychiatric sample from controls. *J. Child Psychol. Psychiatry* **62**, 1079–1089 (2021).

68. Duncan, L. et al. Analysis of polygenic risk score usage and performance in diverse human populations. *Nat. Commun.* **10**, 3328 (2019).

69. Ahern, J., Thompson, W., Fan, C. C. & Loughnan, R. Comparing pruning and thresholding with continuous shrinkage polygenic score methods in a large sample of ancestrally diverse adolescents from the ABCD Study⁺. *Behav. Genet.* **53**, 292–309 (2023).

70. Garavan, H. et al. Recruiting the ABCD sample: design considerations and procedures. *Dev. Cogn. Neurosci.* **32**, 16–22 (2018).

71. Casey, B. J. et al. The Adolescent Brain Cognitive Development (ABCD) study: imaging acquisition across 21 sites. *Dev. Cogn. Neurosci.* **32**, 43–54 (2018).

72. Sollis, E. et al. The NHGRI-EBI GWAS Catalog: knowledgebase and deposition resource. *Nucleic Acids Res.* **51**, D977–D985 (2023).

73. Gadin, J., Zetterberg, R., Meijsen, J. & Schork, A. Cleansumstats: converting GWAS sumstats to a common format to facilitate downstream applications. *Zenodo* <https://zenodo.org/records/7540572> (2023).

74. Uban, K. A. et al. Biospecimens and the ABCD study: rationale, methods of collection, measurement and early data. *Dev. Cogn. Neurosci.* **32**, 97–106 (2018).

75. Baurley, J. W., Edlund, C. K., Pardamean, C. I., Conti, D. V. & Bergen, A. W. Smokescreen: a targeted genotyping array for addiction research. *BMC Genomics* **17**, 145 (2016).

76. Taliun, D. et al. Sequencing of 53,831 diverse genomes from the NHLBI TOPMed Program. *Nature* **590**, 290–299 (2021).

77. Chen, C. Y. et al. Improved ancestry inference using weights from external reference panels. *Bioinformatics* **29**, 1399–1406 (2013).

78. Auton, A. et al. A global reference for human genetic variation. *Nature* **526**, 68–74 (2015).

79. Reich, D. et al. Reconstructing Native American population history. *Nature* **488**, 370–374 (2012).

80. Ge, T., Chen, C. Y., Ni, Y., Feng, Y. A. & Smoller, J. W. Polygenic prediction via Bayesian regression and continuous shrinkage priors. *Nat. Commun.* **10**, 1776 (2019).

81. Chang, C. C. et al. Second-generation PLINK: rising to the challenge of larger and richer datasets. *GigaScience* **4**, 7 (2015).

82. Hagler, D. J. Jr. et al. Image processing and analysis methods for the Adolescent Brain Cognitive Development Study. *NeuroImage* **202**, 116091 (2019).

83. Desikan, R. S. et al. An automated labeling system for subdividing the human cerebral cortex on MRI scans into gyral based regions of interest. *NeuroImage* **31**, 968–980 (2006).

84. Achenbach, T. M. & Ruffle, T. M. The child behavior checklist and related forms for assessing behavioral/emotional problems and competencies. *Pediatr. Rev.* **21**, 265–271 (2000).

85. Achenbach, T. M., Ivanova, M. Y., Rescorla, L. A., Turner, L. V. & Althoff, R. R. Internalizing/externalizing problems: review and recommendations for clinical and research applications. *J. Am. Acad. Child Adolesc. Psychiatry* **55**, 647–656 (2016).

86. Peverill, M. et al. Socioeconomic status and child psychopathology in the United States: a meta-analysis of population-based studies. *Clin. Psychol. Rev.* **83**, 101933 (2021).

87. Rakesh, D., Zalesky, A. & Whittle, S. Assessment of parent income and education, neighborhood disadvantage, and child brain structure. *JAMA Netw. Open* **5**, e2226208 (2022).
88. Fan, C. C., Loughnan, R., Wilson, S. & Hewitt, J. K. Genotype data and derived genetic instruments of Adolescent Brain Cognitive Development Study[®] for better understanding of human brain development. *Behav. Genet.* **53**, 159–168 (2023).
89. Markello, R. D. et al. neuromaps: structural and functional interpretation of brain maps. *Nat. Methods* **19**, 1472–1479 (2022).
90. Savli, M. et al. Normative database of the serotonergic system in healthy subjects using multi-tracer PET. *NeuroImage* **63**, 447–459 (2012).
91. Beliveau, V. et al. A high-resolution *in vivo* atlas of the human brain's serotonin system. *J. Neurosci.* **37**, 120–128 (2017).
92. Radhakrishnan, R. et al. Age-related change in 5-HT₆ receptor availability in healthy male volunteers measured with ¹¹C-GSK215083 PET. *J. Nucl. Med.* **59**, 1445–1450 (2018).
93. Normandin, M. D. Imaging the cannabinoid CB1 receptor in humans with [¹¹C]OMAR: assessment of kinetic analysis methods, test-retest reproducibility, and gender differences. *J. Cereb. Blood Flow Metab.* **35**, 1313–1322 (2015).
94. Kaller, S. et al. Test-retest measurements of dopamine D₁-type receptors using simultaneous PET/MRI imaging. *Eur. J. Nucl. Med. Mol. Imaging* **44**, 1025–1032 (2017).
95. Smith, C. T. et al. Partial-volume correction increases estimated dopamine D2-like receptor binding potential and reduces adult age differences. *J. Cereb. Blood Flow Metab.* **39**, 822–833 (2019).
96. Dukart, J. et al. Cerebral blood flow predicts differential neurotransmitter activity. *Sci. Rep.* **8**, 4074 (2018).
97. Nørgaard, M. et al. A high-resolution *in vivo* atlas of the human brain's benzodiazepine binding site of GABA(A) receptors. *NeuroImage* **232**, 117878 (2021).
98. Gallezot, J. D. Determination of receptor occupancy in the presence of mass dose: [¹¹C]GSK189254 PET imaging of histamine H₃ receptor occupancy by PF-03654746. *J. Cereb. Blood Flow Metab.* **37**, 1095–1107 (2017).
99. Ding, Y. S. PET imaging of the effects of age and cocaine on the norepinephrine transporter in the human brain using (S,S)-[¹¹C]O-methylreboxetine and HRRT. *Synapse* **64**, 30–38 (2010).
100. Naganawa, M. et al. First-in-human assessment of (11)C-LSN3172176, an M1 muscarinic acetylcholine receptor PET radiotracer. *J. Nucl. Med.* **62**, 553–560 (2021).
101. Aghourian, M. Quantification of brain cholinergic denervation in Alzheimer's disease using PET imaging with [¹⁸F]-FEOBV. *Mol. Psychiatry* **22**, 1531–1538 (2017).
102. Smart, K. Sex differences in [¹¹C]ABP688 binding: a positron emission tomography study of mGlu5 receptors. *Eur. J. Nucl. Med. Mol. Imaging* **46**, 1179–1183 (2019).
103. Kantonen, T. et al. Interindividual variability and lateralization of μ-opioid receptors in the human brain. *NeuroImage* **217**, 116922 (2020).
104. Váša, F. & Mišić, B. Null models in network neuroscience. *Nat. Rev. Neurosci.* **23**, 493–504 (2022).

Acknowledgements

This work was supported by the National Institute of Mental Health (K01MH136403 to H.Z., R01MH122688 to C.C.F. and R01MH128959 to C.C.F. and W.K.T.). The funding sources had no role in the design and conduct of the study; collection, management, analysis and interpretation of the data; preparation, review or approval of the manuscript; and decision to submit the manuscript for publication. Data used in the preparation of this article were obtained from the Adolescent Brain Cognitive Development (ABCD) Study

(<https://abcdstudy.org>), held in the NIMH Data Archive (NDA). This is a multisite, longitudinal study designed to recruit more than 10,000 children aged 9–10 and follow them over 10 years into early adulthood. The ABCD Study is supported by the National Institutes of Health and additional federal partners under award numbers U01DAO41048, U01DA050989, U01DA051016, U01DAO41022, U01DAO51018, U01DAO51037, U01DAO50987, U01DAO41174, U01DAO41106, U01DAO41117, U01DAO41028, U01DAO41134, U01DAO50988, U01DAO51039, U01DAO41156, U01DAO41025, U01DAO41120, U01DAO51038, U01DAO41148, U01DAO41093, U01DAO41089, U24DA041123 and U24DA041147. A full list of supporters is available at <https://abcdstudy.org/federal-partners.html>. A listing of participating sites and a complete listing of the study investigators can be found at https://abcdstudy.org/consortium_members/. ABCD consortium investigators designed and implemented the study and/or provided data but did not necessarily participate in analysis or writing of this report. This paper reflects the views of the authors and may not reflect the opinions or views of the NIH or ABCD consortium investigators.

Author contributions

Conception and design of work: H.Z., C.C.F. and W.K.T. Data acquisition and analysis: H.Z., J.A., R.J.L., F.N., B.X., K.L.F., R.L.A., M.P.P., C.C.F. and W.K.T. Interpretation of results: H.Z., J.S., E.H., L.M.W., M.P.P., C.C.F. and W.K.T. Drafting paper: H.Z. Revision of paper: H.Z., J.S., E.H., J.A., R.J.L., F.N., B.X., K.L.F., R.L.A., L.M.W., M.P.P., C.C.F. and W.K.T. Funding: H.Z., C.C.F. and W.K.T.

Competing interests

The authors declare no competing interests.

Additional information

Supplementary information The online version contains supplementary material available at <https://doi.org/10.1038/s44220-026-00585-w>.

Correspondence and requests for materials should be addressed to Haixia Zheng.

Peer review information *Nature Mental Health* thanks Nicole Karcher, Claire Niedzwiedz and the other, anonymous, reviewer(s) for their contribution to the peer review of this work.

Reprints and permissions information is available at www.nature.com/reprints.

Publisher's note Springer Nature remains neutral with regard to jurisdictional claims in published maps and institutional affiliations.

Open Access This article is licensed under a Creative Commons Attribution 4.0 International License, which permits use, sharing, adaptation, distribution and reproduction in any medium or format, as long as you give appropriate credit to the original author(s) and the source, provide a link to the Creative Commons licence, and indicate if changes were made. The images or other third party material in this article are included in the article's Creative Commons licence, unless indicated otherwise in a credit line to the material. If material is not included in the article's Creative Commons licence and your intended use is not permitted by statutory regulation or exceeds the permitted use, you will need to obtain permission directly from the copyright holder. To view a copy of this licence, visit <http://creativecommons.org/licenses/by/4.0/>.

© The Author(s) 2026

Reporting Summary

Nature Portfolio wishes to improve the reproducibility of the work that we publish. This form provides structure for consistency and transparency in reporting. For further information on Nature Portfolio policies, see our [Editorial Policies](#) and the [Editorial Policy Checklist](#).

Statistics

For all statistical analyses, confirm that the following items are present in the figure legend, table legend, main text, or Methods section.

n/a Confirmed

- The exact sample size (n) for each experimental group/condition, given as a discrete number and unit of measurement
- A statement on whether measurements were taken from distinct samples or whether the same sample was measured repeatedly
- The statistical test(s) used AND whether they are one- or two-sided
Only common tests should be described solely by name; describe more complex techniques in the Methods section.
- A description of all covariates tested
- A description of any assumptions or corrections, such as tests of normality and adjustment for multiple comparisons
- A full description of the statistical parameters including central tendency (e.g. means) or other basic estimates (e.g. regression coefficient) AND variation (e.g. standard deviation) or associated estimates of uncertainty (e.g. confidence intervals)
- For null hypothesis testing, the test statistic (e.g. F , t , r) with confidence intervals, effect sizes, degrees of freedom and P value noted
Give P values as exact values whenever suitable.
- For Bayesian analysis, information on the choice of priors and Markov chain Monte Carlo settings
- For hierarchical and complex designs, identification of the appropriate level for tests and full reporting of outcomes
- Estimates of effect sizes (e.g. Cohen's d , Pearson's r), indicating how they were calculated

Our web collection on [statistics for biologists](#) contains articles on many of the points above.

Software and code

Policy information about [availability of computer code](#)

Data collection	This study used data from the Adolescent Brain Cognitive Development (ABCD) Study, curated release 5.1. These data are publicly available through the National Institute of Mental Health Data Archive (NDA) under the ABCD collection (https://ndar.nih.gov/abcd). Access requires completion of the NDA Data Use Certification.
Data analysis	No custom algorithms were developed for this study. Analyses were performed using publicly available software, including PLINK 2.0 and PRS-CS for genetic analyses; FreeSurfer v7.1.1 for neuroimaging processing; and R (version 4.4.1) with the packages nlme (v3.1-168), metafor (v4.8-0), and lavaan (v0.6-19) for statistical modelling and mediation analyses. Neurobiological annotation was conducted using the Neuromaps toolbox. All software used in this study is freely accessible.

For manuscripts utilizing custom algorithms or software that are central to the research but not yet described in published literature, software must be made available to editors and reviewers. We strongly encourage code deposition in a community repository (e.g. GitHub). See the Nature Portfolio [guidelines for submitting code & software](#) for further information.

Data

Policy information about [availability of data](#)

All manuscripts must include a [data availability statement](#). This statement should provide the following information, where applicable:

- Accession codes, unique identifiers, or web links for publicly available datasets
- A description of any restrictions on data availability
- For clinical datasets or third party data, please ensure that the statement adheres to our [policy](#)

This study used data from the Adolescent Brain Cognitive Development (ABCD) Study, curated release 5.1. These data are publicly available through the National Institute of Mental Health Data Archive (NDA) under the ABCD collection (<https://nda.nih.gov/abcd>). Access requires completion of the NDA Data Use Certification.

Research involving human participants, their data, or biological material

Policy information about studies with [human participants or human data](#). See also policy information about [sex, gender \(identity/presentation\), and sexual orientation](#) and [race, ethnicity and racism](#).

Reporting on sex and gender

Sex at birth (male/female) was collected via parent report in the ABCD Study and included as a fixed-effect covariate in all analyses. Sex was considered in study design and analyses because it is known to influence neurodevelopment and health outcomes. Gender identity was not collected or analyzed in this dataset. Findings apply to participants of all sexes combined, as no sex-stratified analyses were conducted; the lack of sex-specific models reflects the study's focus on genetic and neurodevelopmental effects rather than sex differences. Disaggregated sex data are available in the ABCD dataset, and all data were collected with parental consent and child assent.

Reporting on race, ethnicity, or other socially relevant groupings

Race/ethnicity, parental education, and household income were included as fixed-effect covariates in analyses. Parental education and household income, which were reported by the child's guardian, are key indicators of socioeconomic status, which is known to be associated with neurodevelopmental trajectories and psychopathology.

Population characteristics

Age, body mass index (BMI), and the first ten principal components of ancestry were included as fixed-effect covariate in analyses. These variables are well-established correlates of both systemic inflammation and/or brain structure, and therefore help reduce residual confounding.

Recruitment

Recruitment was conducted primarily through public and private elementary schools using a probability sampling approach stratified by age, sex, race/ethnicity, socioeconomic status, and urbanicity, with targeted oversampling of underrepresented groups (e.g., African American, Hispanic, and rural youth) to better reflect the U.S. population. The participating schools were drawn from each site's catchment area, collectively encompassing ~20% of the U.S. population of 9–10-year-olds. Approximately 9.6% of contacted families enrolled, yielding a cohort broadly representative of the sociodemographic composition of U.S. children. Enrollment demographics were monitored throughout recruitment, and later school samples were dynamically adjusted to correct deviations from target demographics. Approximately half of the sample was enriched for children showing early signs of externalizing or internalizing symptoms to ensure sufficient power for studying developmental risk trajectories.

Ethics oversight

Institutional Review Board (IRB)

Note that full information on the approval of the study protocol must also be provided in the manuscript.

Field-specific reporting

Please select the one below that is the best fit for your research. If you are not sure, read the appropriate sections before making your selection.

Life sciences Behavioural & social sciences Ecological, evolutionary & environmental sciences

For a reference copy of the document with all sections, see nature.com/documents/nr-reporting-summary-flat.pdf

Behavioural & social sciences study design

All studies must disclose on these points even when the disclosure is negative.

Study description

Quantitative, observational, longitudinal cohort study using secondary neuroimaging, genetic, and behavioral data.

Research sample

This longitudinal cohort study used data from the Adolescent Brain Cognitive Development (ABCD) Study, a nationwide study of 11,868 youth aged 9–10 years at baseline recruited from 21 U.S. sites. At baseline, the mean age was 9.91 years and 11.95 years at follow-up (Year 2); 47.5% of participants at baseline and 45.9% at Year 2 were female. The mean BMI increased from 18.73 (SD = 3.96) to 20.49 (SD = 4.45). Participants self-identified as White (52.8%), Black (14.9%), Hispanic (19.8%), Asian (1.9%), or Multiracial (10.6%). Parental education and household income distributions reflected broad socioeconomic diversity. The cohort is broadly representative of U.S. children aged 9–10 years, and data were obtained from the National Institute of Mental Health Data Archive (NDA; ABCD Release 5.1).

Sampling strategy

Participants were recruited through public and private elementary schools using a probability sampling approach stratified by age, sex, race/ethnicity, socioeconomic status, and urbanicity, with oversampling of underrepresented groups to enhance representativeness of the U.S. population. Of the 11,868 participants in the original ABCD cohort, 140 with missing baseline MRI data, 476 with missing PGS_CRP data, 36 from a site that withdrew, and 2 with missing genetic ancestry data were excluded, yielding a final analytic sample of 11,214. Participants were stratified by genetic ancestry (European [n = 6,336] vs. non-European [n = 4,878]) based on genetic ancestry score thresholds (≥ 0.8 vs. < 0.8) to mitigate population stratification bias. No formal sample-size calculation was performed; the ABCD cohort's large, nationally representative design and multi-site recruitment were determined a priori to ensure adequate statistical power to detect small-to-medium effects in developmental and neurobiological outcomes. Within each ancestry group, the majority of participants (European n = 4,588; non-European n = 3,158) completed both baseline and Year 2 assessments. Meta-analytic methods were used to integrate findings across ancestry groups, enhancing generalizability of results.

Data collection

This study used secondary data from the Adolescent Brain Cognitive Development (ABCD) Study, which collected data at 21 U.S. sites using standardized protocols. Trained research staff administered parent- and youth-report questionnaires and acquired 3T MRI scans (Siemens, GE, and Philips systems) following harmonized procedures. All data underwent centralized quality control by the ABCD Data Analysis and Informatics Resource Center and were obtained in de-identified form from the National Institute of Mental Health Data Archive (NDA; ABCD Release 5.1). The present investigators did not participate in data collection.

Timing

09/01/2016 - 02/15/2021

Data exclusions

The ABCD Study excluded participants for non-fluency in English, absence of a guardian fluent in English or Spanish, major medical or neurological conditions, gestational age < 28 weeks or birthweight $< 1,200$ grams, MRI contraindications, history of traumatic brain injury, current schizophrenia, moderate to severe autism spectrum disorder, intellectual disability, or alcohol/substance use disorder.

For the current analysis, the baseline cohort excluded 140 participants missing MRI data, 476 missing PGS_CRP data, 36 screened at a study site that withdrew, and 2 missing genetic ancestry data, yielding 11,214 participants. The two-year follow-up cohort excluded 2,881 with missing MRI data, 267 missing PGS_CRP data, and 2 missing genetic ancestry data.

Non-participation

Of 11,214 participants at baseline, 7,823 completed the two-year follow-up, reflecting a 70% retention (30% attrition) rate.

Randomization

Participants were not randomized; this was an observational study. Analyses controlled for key covariates (age, sex, BMI, socioeconomic factors, and ancestry components) and stratified by genetic ancestry to reduce bias.

Reporting for specific materials, systems and methods

We require information from authors about some types of materials, experimental systems and methods used in many studies. Here, indicate whether each material, system or method listed is relevant to your study. If you are not sure if a list item applies to your research, read the appropriate section before selecting a response.

Materials & experimental systems

n/a	Involved in the study
<input checked="" type="checkbox"/>	<input type="checkbox"/> Antibodies
<input checked="" type="checkbox"/>	<input type="checkbox"/> Eukaryotic cell lines
<input checked="" type="checkbox"/>	<input type="checkbox"/> Palaeontology and archaeology
<input checked="" type="checkbox"/>	<input type="checkbox"/> Animals and other organisms
<input checked="" type="checkbox"/>	<input type="checkbox"/> Clinical data
<input checked="" type="checkbox"/>	<input type="checkbox"/> Dual use research of concern
<input checked="" type="checkbox"/>	<input type="checkbox"/> Plants

Methods

n/a	Involved in the study
<input checked="" type="checkbox"/>	<input type="checkbox"/> ChIP-seq
<input checked="" type="checkbox"/>	<input type="checkbox"/> Flow cytometry
<input type="checkbox"/>	<input checked="" type="checkbox"/> MRI-based neuroimaging

Plants

Seed stocks

NA

Novel plant genotypes

NA

Authentication

NA

Magnetic resonance imaging

Experimental design

Design type

The ABCD MRI protocol included both resting-state and task-based fMRI. The task-based scans used event-related designs for the Monetary Incentive Delay (MID) and Stop Signal Task (SST), and a block design for the emotional n-back (EN-back) working memory task. Details are not repeated in the main text to avoid redundancy, but are fully described in the ABCD imaging acquisition papers cited in the manuscript (Refs. 44 and 56).

Design specifications

Each session included two resting-state fMRI runs (~5 min each) and three task-based paradigms (MID, SST, EN-back). MID: event-related; ~50 trials per run (2 runs); 4–6 s trial duration; jittered 1.5–4 s inter-trial interval. SST: event-related; 180 trials per run (2 runs), including ~30 stop trials (16.7%); 1 s trial duration; 1.7–3 s inter-trial interval. EN-back: block design; 8 blocks per run (2 runs) alternating 0-back and 2-back; ~30 s per block with 15–20 s fixation between blocks. Details are not repeated in the main text to avoid redundancy, but are fully described in the ABCD imaging acquisition papers cited in the manuscript (Refs. 44 and 56).

Behavioral performance measures

Behavioral data were collected using computerized response boxes during all task-based fMRI scans. MID: accuracy (hit rate) and reaction time. SST: stop-signal reaction time (SSRT), accuracy on “Go” and “Stop” trials. EN-back: accuracy and reaction time on 0-back and 2-back blocks. Mean accuracy and reaction times across participants confirmed expected task engagement and performance consistency. Details are not repeated in the main text to avoid redundancy, but are fully described in the ABCD imaging acquisition papers cited in the manuscript (Refs. 44 and 56).

Acquisition

Imaging type(s)

Structural MRI (T1-weighted), functional MRI (resting-state and task-based fMRI), and diffusion MRI.

Field strength

3 Tesla

Sequence & imaging parameters

Detailed MRI acquisition parameters (e.g., TR, TE, TI, voxel size, sequence type, and field strength) are specified in the ABCD Study protocol, which our analyses followed exactly (references 44 and 56 in the manuscript). Therefore, acquisition details are not repeated in the main text but are available in the cited ABCD documentation

Area of acquisition

Whole brain coverage, including cerebrum and cerebellum.

Diffusion MRI

Used

Not used

Parameters Multi-shell diffusion MRI was acquired using a single-shot, spin-echo EPI sequence with 96 diffusion directions across four b-values (500, 1000, 2000, and 3000 s/mm²), plus 7 interspersed b0 volumes. The sequence used no cardiac gating. (standardized ABCD Study diffusion protocol, Refs 44 and 56)

Preprocessing

Preprocessing software

ABCD pipeline implemented in FreeSurfer v7.1.1, FSL, and AFNI, managed by the ABCD Data Analysis and Informatics Resource Center (DAIRC).

Normalization

Images were aligned to the participant’s native space and then normalized to MNI152 standard space.

Normalization template

Montreal Neurological Institute (MNI152) atlas.

Noise and artifact removal

Gradient nonlinearity distortion correction, B0 inhomogeneity correction, motion correction, and intensity normalization performed as part of the ABCD preprocessing pipeline. fMRI data underwent ICA-based artifact removal (ICA-FIX) and nuisance regression to reduce motion and physiological noise.

Volume censoring

Volumes with framewise displacement >0.9 mm were censored from fMRI analyses; participants with >50% of frames censored were excluded, per ABCD preprocessing standards.

Statistical modeling & inference

Model type and settings

Linear mixed-effects models tested associations between PGS_CRP, age, and early-life infection, including random intercepts for individual, family, and site. Continuous predictors were standardized.

Effect(s) tested

Main and interaction effects of PGS_CRP × age × early-life infection on cortical thickness and psychopathology. Structural equation models (SEM) tested cortical thinning as a mediator of PGS_CRP effects.

Specify type of analysis:

Whole brain

ROI-based

Both

Anatomical location(s)	Anatomical regions were defined using the Desikan–Killiany cortical atlas, applied through automated surface-based labeling in FreeSurfer v7.1.1 to derive 34 cortical regions per hemisphere and global mean cortical thickness measures.
Statistic type for inference (See Eklund et al. 2016)	Voxel-wise statistical inference was performed within each ROI, with results corrected for multiple comparisons using False Discovery Rate (FDR; $p < 0.05$, two-tailed) across all tested regions. No cluster-wise correction was applied.
Correction	Multiple comparisons were controlled using the False Discovery Rate (FDR) at $p < 0.05$ (two-tailed) across all cortical regions.

Models & analysis

n/a	Involved in the study
<input checked="" type="checkbox"/>	<input type="checkbox"/> Functional and/or effective connectivity
<input checked="" type="checkbox"/>	<input type="checkbox"/> Graph analysis
<input type="checkbox"/>	<input checked="" type="checkbox"/> Multivariate modeling or predictive analysis
Multivariate modeling and predictive analysis	Independent variable: PGS_CRP (polygenic score for C-reactive protein). Feature extraction: Global mean cortical thickness change (T2–T0) derived from FreeSurfer parcellations. Dimension reduction: Not applicable (single global mediator variable). Model: Structural equation modeling (SEM) tested indirect effects of PGS_CRP on psychopathology via cortical thickness change. Evaluation metrics: Standardized path coefficients, bootstrapped confidence intervals (1,000 samples), and model fit indices (CFI, TLI, SRMR).